Document downloaded from:

http://hdl.handle.net/10251/183676

This paper must be cited as:

Gutiérrez-Tarriño, S.; Gaona Miguélez, JA.; Oña-Burgos, P. (2021). Tailoring the electron density of cobalt oxide clusters to provide highly selective superoxide and peroxide species for aerobic cyclohexane oxidation. Dalton Transactions. 50(42):15370-15379. https://doi.org/10.1039/d1dt02347k

The final publication is available at

https://doi.org/10.1039/d1dt02347k

Copyright The Royal Society of Chemistry

Additional Information

Tailoring the Electron Density of Cobalt Oxide Clusters to Provide High Selective Superoxide and Peroxide Species for Aerobic Cyclohexane Oxidation

Silvia Gutiérrez-Tarriño,[a] José Gaona-Miguélez[a] and Pascual Oña-Burgos*[a,b]

[a] Instituto de Tecnología Química, Universitat Politècnica de València-Consejo Superior de Investigaciones Científicas (UPV-CSIC), Avda. de los Naranjos s/n, 46022 Valencia, Spain.

[b] Department of Chemistry and Physics, Research Centre CIAIMBITAL, University of Almería, Ctra. Sacramento, s/n, 04120 Almería, Spain.

Abstract

A family of cobalt clusters, where their electronic properties can be modulated, has been developed. These cobalt clusters are highly active and selective for the aerobic cyclohexane oxidation, whose reaction mechanism is discussed on the basis of kinetics and spin trapping experiments. Moreover, in-situ Raman spectroscopy was used to characterize the oxygen species formed on the cobalt cluster during the oxidation reaction. The catalytic activity and the species formed in the reaction media have been correlated with the cluster electronic density, and the product distribution has been related to the reaction pathway promoted, which has been clearly associated with the electron density of the catalysts.

1. Introduction

In the quest for economic and sustainable global carbon management, hydrocarbons have become a main raw material. In this sense, selective oxidation of hydrocarbons is an important research area both in industry and academia.[1–4] One of the most challenging subjects in this topic is the catalytic and selective aerobic oxidation of alkanes and cycloalkanes to alcohols, aldehydes and ketones.[5] Since the associated bond energies for the CH bonds is high,[6] and the formed products can be more easily oxidized, selectivity becomes the key issue during the oxidation of these molecules.[7–9]

More specifically the oxidation of cyclohexane to cyclohexanone and cyclohexanol (KA-oil) is of great industrial interest,[10] as they these are precursors of ε-caprolactam and adipic acid. These are building blocks of the nylon-6 and nylon-6-6 polymers, respectively, and over one billion tons of ciclohexanol and cyclohexanone are produced every year worldwide.[1,11] Nevertheless, as already said, cyclohexanol and cyclohexanone are more reactive than the reactant, cyclohexane, and the selectivity of the process strongly decreases when increasing the conversion. In fact, the

industry employs cobalt complexes as catalysts[12] to achieve high selectivity (about 80%) of KA-oil but cyclohexane conversion is normally below 9%.

Recently, the raising of environmental concerns has led to use air as oxidant under mild conditions and to avoid the wasteful addition of oxidation agents and solvents. Over recent decades, all type of catalysts have been reported for the liquid-phase cyclohexane oxidation; organometallic complexes[13], metal-organic frameworks[14,15], carbon materials[16,17], silica[18,19] and zeolites[20]. However, they are mostly used in combination with additives in solvents, under severe conditions or with hydroperoxides as oxidizing agents. Therefore, a suitable and sustainable catalyst for this process should be active and selective in neat conditions using air as oxidant (instead of molecular oxygen) and without any additional oxidation agents under mild conditions.

The development of the cobalt cluster $[Co_4O_4(OAc)_4py_4]$ by Beattie et al[21] has given rise to several works by independent research groups. For instances, this cobalt cluster has driven force the formation of new materials based on metal-organic frameworks (MOFs) employing conventional organic linkers.[22,23] Besides, Dismukes' group has implemented the cobalt cluster $[Co_4O_4(OAc)_4py_4]$ as a mimetic of the PSII in the water oxidation step, where oxygen is formed together with electrons and protons.[24] Moreover, Tilley´s group has observed the mechanism of the O-O bond formation by using this cluster, and some intermediates such as hydroxy **B**, terminal oxo **C**, hydroperoxide **D** and peroxide radicals **E** were observed (Scheme 1a).[25] These types of species are essential to promote CH activation in the less reactive alkanes. In fact, the mechanism of O_2 activation for CH bond oxidation by hemo-catalysts is also based on these types of intermediates (Scheme 1b).[26] In addition, Das and co-workers have briefly used $[Co_4O_4(OAc)_4py_4]$ for the aerobic oxidation of activated CH bonds of ethylbenzene and *p*-xylene.[27]

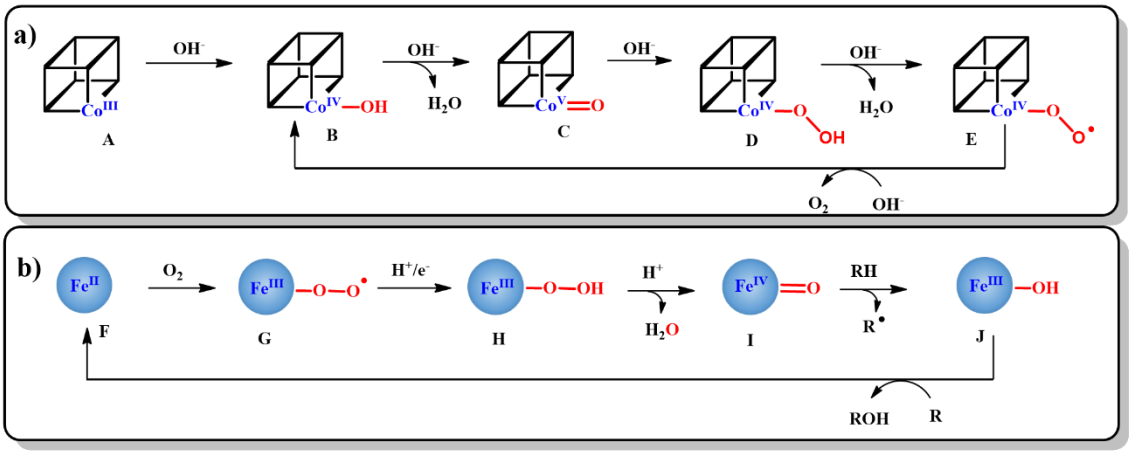

Scheme 1. a) O-O bond formation mechanism by using $[Co_4O_4(OAc)_4py_4]$. b) O_2 activation mechanism for CH bond oxidation by hemo-catalysts.

Considering the previous issues exposed herein, the synthesis of well-defined tetranuclear cobalt oxoclusters $[Co_4O_4(RCO_2)_4py^*_4]$ has been carried out by modulation of the electronic density with the type of carboxylate and by introducing different substituents in the *para* position of the pyridine ring. Then, these clusters have been studied for the aerobic oxidation of cyclohexane in neat conditions, using nitrogen enriched air (with a low content of oxygen, 5%) as oxidant, showing high activity and selectivity under non-severe conditions. Moreover, a mechanistic study of the reaction has been carried out by spin-trapping, kinetic experiments and Raman spectroscopy in order to identify oxidant intermediates, which are controlled by the electronic density of the clusters. Finally, based on the experimental results and in-situ studies, a plausible mechanism has been proposed.

2. Results and discussion

2.1 Synthesis and characterization

Cobalt cubane catalysts **1**-**6** with different carboxylate and pyridine ligands were prepared using a reported method (Scheme 2a).[25] The detailed procedures for the catalyst are given in the Supporting Information. The disadvantage of this synthetic method is that the oxidation conditions limit the use of some bifunctional ligands. Therefore, a straightforward procedure based on carboxylate exchange using **1**-**3** as precursors and benzoic acid as reagent has been developed to achieve clusters **4**-**6** in high yields (Scheme 2b). The driving force in this ligand exchange method is the difference of pK_b between the two carboxylate groups, pK_b 9.24 and 9.81 for the acetate and benzoate, respectively.

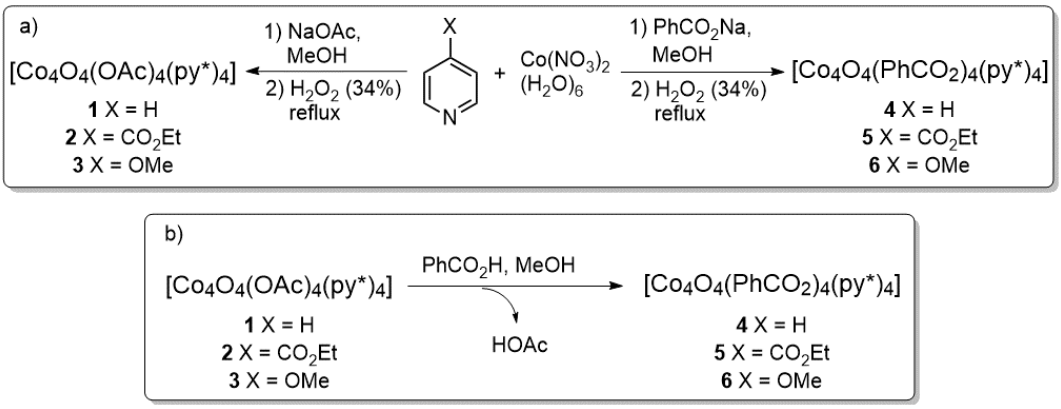

Scheme 2. a) General synthetic scheme of tetranuclear cobalt clusters **1**-**6**. b) Synthesis of cobalt clusters **4**-**6** employing clusters **1**-**3** as building blocks.

These cobalt clusters **1**-**6** have been fully characterized by several techniques such as X-ray diffraction (Figure 1), CV (Figures S1-S3), NMR (Figures S4-S15), ESI-MS (Figures S16-S21), EA and ICP. The techniques and characterization data are described in the Supporting Information

and the characterization data reported in the literature for the known clusters was used for comparison.[27–29] In this sense, suitable crystals for single-crystal X-ray diffraction were obtained for the clusters **2**, **5** and **6**. A perspective view of clusters **2**, **5** and **6** is illustrated in Figure 1. Some important distances and angles of each complex are indicated in Table 1 (more information in Table S1).

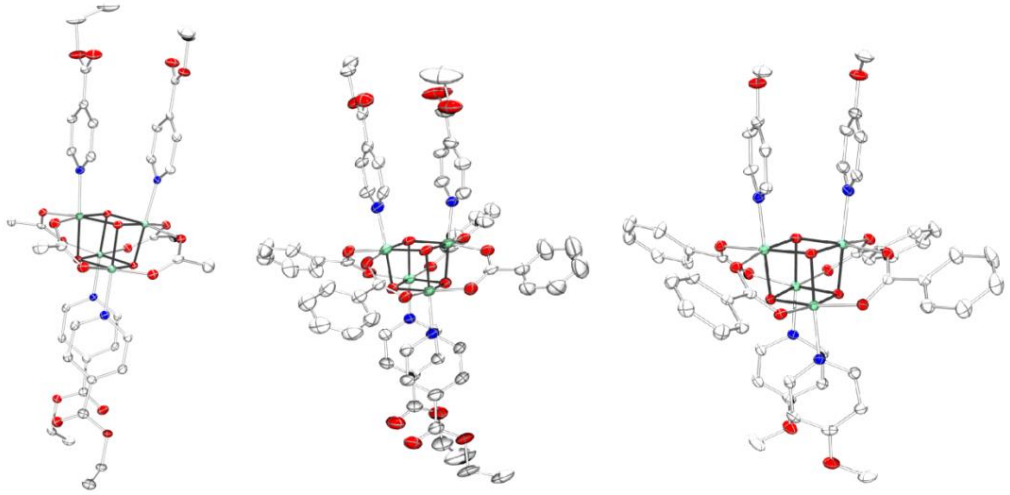

Figure 1. X-Ray structure of complexes **2**, **5** and **6**, respectively. Hydrogen atoms are omitted for clarity.

Table 1. Average Interatomic Bond Distances (Å) and angles (deg) for **2, 5** and **6** complexes compared with **1** and **4**.

Bond Distances (Å) and angles (deg)	**2**	**5**	**6**	**1**[27]	**4**[30]
Co – N (py) (Å)	1.964	1.959	1.958	1.962	1.968
Co – (μ_3-O) (Å)	1.867	1.864	1.868	1.865	1.879
Co – O_{carbox}(Å)	1.949	1.952	1.956	1.953	1.967
Co···Co[a](Å)	2.835	2.829	2.824	2.815	2.856
Co···Co[b](Å)	2.701	2.690	2.701	2.702	2.725
O – Co – O[c] (deg)	84.74	84.88	85.08	85.21	84.80
Co – O – Co[c] (deg)	94.81	94.66	94.51	94.97	94.69

[a]Bridged by two oxo ligands only. [b]Bridged by two oxo ligands and a bidentate carboxylate. [c]Only oxygen atoms of the Co_4O_4 core are consider.

The structural features obtained by single-crystal X-ray diffraction lead to conclude that bond lengths in Co(III)-O(oxide) and Co(III)-O(carboxylate) are in the narrow ranges of 1.848-1.884 and 1.928-1.979 Å, respectively. The carboxylate group bridging two Co(III) strengthens the cubane structure. There are two types of Co-Co distances: one close to 2.83 Å when Co-Co is bridged by only two oxo ligands, and another larger than 2.70 Å when Co-Co are bridged by two

oxo ligands and a bidentate carboxylate ligand. These results are in consonance with related cobalt(III) complexes having a $[Co_4(\mu_3\text{-}O)_4]$ arrangement (vide infra).[27,30] Moreover, the average Co-N distance is in the order of 1.96 Å and the dihedral angles between two pyridines are between 170 and 180º. Thus, the isolated $[Co_4O_4]$ cubanes have the complete cuboidal structure stabilized by two pyridyl-pyridyl stacks.

2.2. Electrochemical characterization

It is well known that the electrochemical properties of cobalt cubane complexes can be modulated by changing the bridging carboxylate ligand and/or the *para*-substituents of the pyridine ligand.[28,31–33] In this sense, the redox potential of **1-6** cubane clusters has been studied by cyclic voltammetry using a three-electrode assembly. The cyclic voltammograms obtained at different scan rates for complexes **1-6** are shown in Figures S1-S3. Chart 1 summarizes the collected data for the generated clusters. On one hand, clusters **3** and **6** with a methoxy group as electron donating group (EDG) in the *para* position of the pyridine ring have associated $E_{1/2}$ of 0.670 and 0.743 V, respectively. On the other hand, clusters **2** and **5**, with an ester as electron withdrawing group (EWG) in the *para* position of the pyridine ring, have associated $E_{1/2}$ of 0.857 and 0.956 V, respectively. Finally, clusters **1** and **4**, with H in the *para* position have associated intermediate values ($E_{1/2}$ of 0.704 and 0.783 V, respectively).

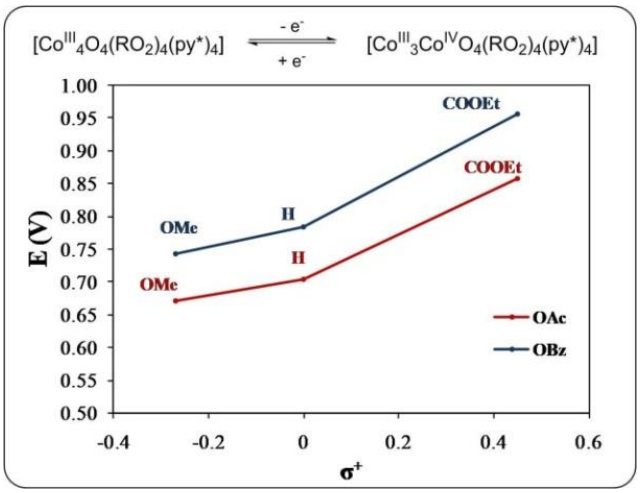

Chart 1. Oxidation potential data for clusters **1-6**. These data are correlated with σ^+ values for the Hammet equation.

Based on that, it can be said that EDG promotes the oxidability of the cobalt cluster from $[(CoIII)_4(\mu_3\text{-}O)_4]^{4+}$ to $[(CoIII)_3Co^{IV}(\mu_3\text{-}O)_4]^{5+}$ while the EWG has the opposite behavior. In addition, acetate substituent also promotes oxidability versus benzoate. Therefore, the electronic properties of the cobalt core can be easily modulated with the selected substituent on the pyridine ring or the carboxylate.

2.3 Catalytic study on cyclohexane oxidation

As stated before, cobalt complexes are well-known catalysts for aerobic alkane and cycloalkane oxidation.[12] Considering that the species identified during water oxidation with cobalt cubanes (Scheme 1a)[25] are directly correlated with the species found in O_2 activation for CH oxidation with hemo-catalysts (Scheme 1b)[26], the synthesized cobalt clusters **1-6** were evaluated as catalysts in the aerobic oxidation of cyclohexane (the detailed procedures for the catalytic study are given in Supporting Information). After optimizing the reaction conditions (Table S2), the reaction temperature was fixed to 130 ºC, and the partial pressure of oxygen was set to 6 bar (ratio N_2:O_2 of 95:5). The results attained under the optimized experimental conditions are summarized in Figure 2 (see results in table S3).

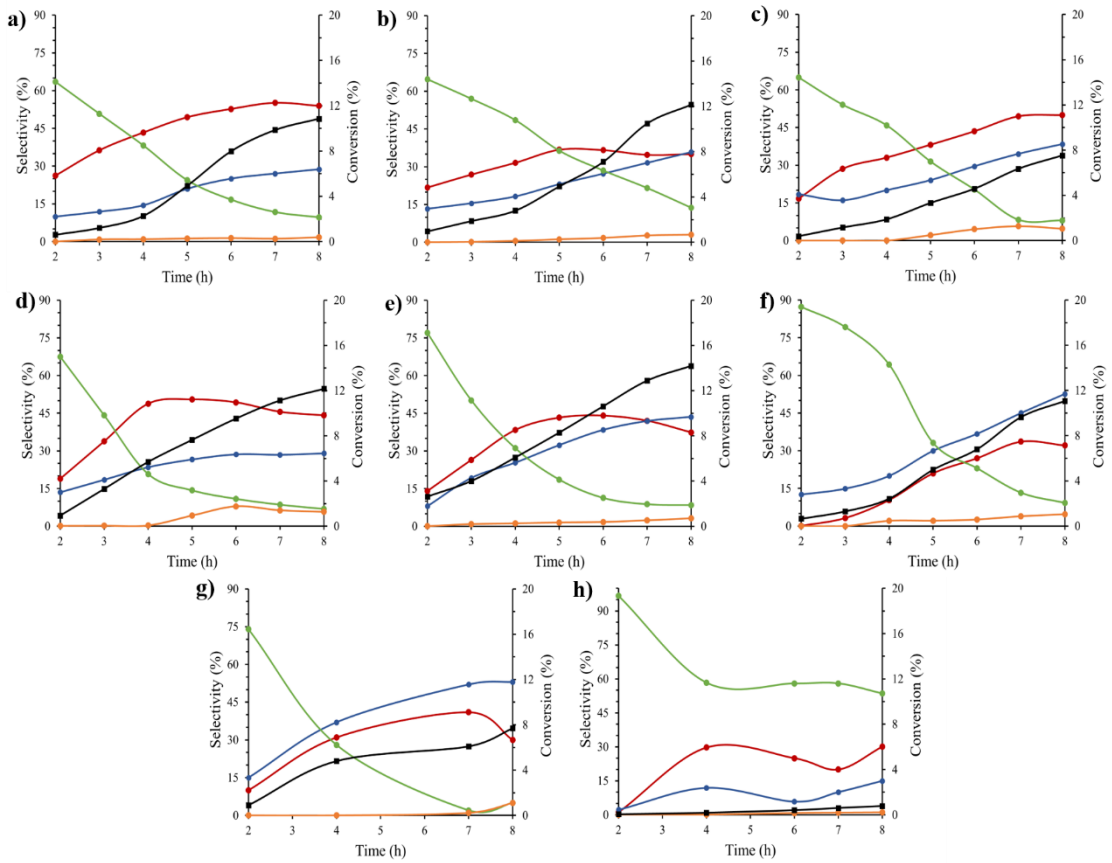

Figure 2. Summary of the catalytic activity in cyclohexane oxidation of a) **1**, b) **2**, c) **3**, d) **4**, e) **5**, f) **6**, g) $Co(OAc)_2$ and h) blank. Reaction conditions: 3g cyclohexane (36 mmol), 0.14 ppm of cobalt, 130 ºC, 6 bar (N_2:O_2 = 95:5), Q = 10 mL/min). Black: total conversion (right axis), red: cyclohexanol, blue: cyclohexanone, green: CHHP and orange: adipic acid (left axis).

Cobalt (II) acetate was initially tested as a benchmark for investigating the activity of cobalt (II) species (Figure 2g). From this study, it could be observed that the catalytic activity of clusters **1-6** (Figure 2a-2f) is better than the one obtained for $Co(OAc)_2$. Thus, these mild conditions highlight the catalytic differences of the synthesized cubane catalysts. Regarding the catalytic

activity, results in Figure 2 show that cobalt clusters decompose less CHHP than $Co(OAc)_2$, and that ol/one ratios are higher for the obtained clusters, whereas $Co(OAc)_2$ promotes the formation of more than 50% of cyclohexanone. To compare the activity of all the catalysts studied in this process, the kinetics of the reaction are plotted, considering both the conversion of cyclohexane and the total selectivity to the desired products (Figure 3a).

According to the cyclic voltammetry results presented before, the catalytic results obtained with clusters **1-6** can be correlated with the electronic properties of each cluster (Figure 3b). That means that catalysts with a higher oxidation potential are more active one and present higher reaction rates. So, an EWG in the *para* position of the pyridine ring promotes higher oxidation potential and, therefore, a higher catalytic activity of the cluster. While an EDG in the *para* position of the pyridine ring promotes lower oxidation potential and, consequently, a lower catalytic activity of the resultant catalyst. These results indicate that cluster **5** is the best catalyst of the cubane series, and also that all cobalt cubanes are clearly better than $Co(OAc)_2$. In fact, the conversion and the selectivity obtained with catalyst **5** show that this is a promising catalyst for this reaction compared to other well-known cobalt complexes.[12]

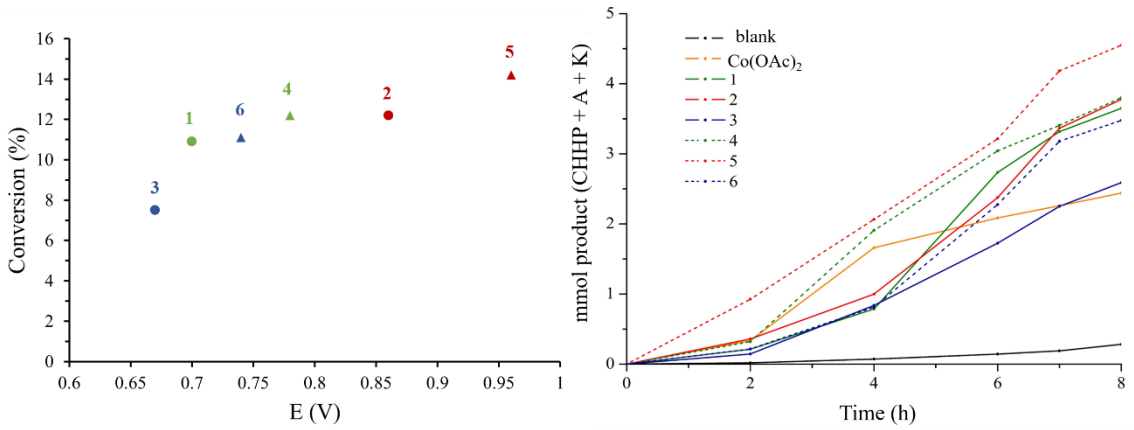

Figure 3. a) Kinetic study for cyclohexane oxidation with cobalt catalysts **1-6**. b) Correlation between conversion and oxidation potential of each cluster.

Moreover, conversion and selectivity values of cobalt cluster catalysts **1-6** (under similar reaction conditions) are ranked within the best catalysts, and there is a clear improvement of most of the materials previously reported (see Table S4) for this particular reaction. In this sense, Chart 2 covers this comparison between catalysts **1-6** to others previously described.

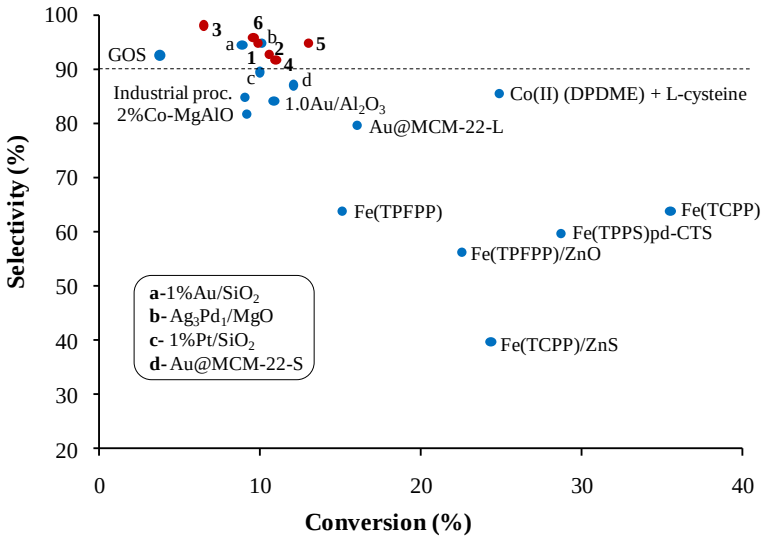

Chart 2. Comparison of **1-6** cobalt catalysts (red) with other reported catalysts (blue) for aerobic cyclohexane oxidation under similar reaction conditions.

2.4 Mechanistic study of the cyclohexane oxidation

In order to correlate the electronic density of the developed catalysts with the generated oxidant intermediates and their catalytic activity, a wide study based on experimental data and *in situ* experiments has been carried out. The elementary reactions involved in the cyclohexane oxidation have a well-established mechanism and these are illustrated in Scheme 3. Reaction **A** implies the formation of cyclohexyl radicals by mediation of organic molecules or metals. Reactions **B** and **C** are the propagation steps, while reaction **D** is the termination of the radical process forming one molecule of cyclohexanol, other of cyclohexanone and one of molecular oxygen. Besides, reactions **Ea** and **Eb** could also improve the propagation step and therefore enhance the reaction rate. Reaction **Ea** is based on heterolytic O-O bond cleavage of CHHP to afford proton radical and cyclohexyl peroxo radical, which can react with cyclohexane following reaction 3 in propagation step. However, reaction **Eb** supposes a homolytic O-O bond of CHHP to promote hydroxy and alkoxy radicals. Both species can react with cyclohexane, reactions **F** and **G**, respectively, to form cyclohexyl radical together with water or cyclohexanol. Although, these species can also improve propagation, these (without any stabilization) are more reactive than peroxo and therefore less selective during proton abstraction. Therefore, the aim of this study is to identify the role of the cobalt cluster in each single step of the whole process and its dependance on the electronic properties.

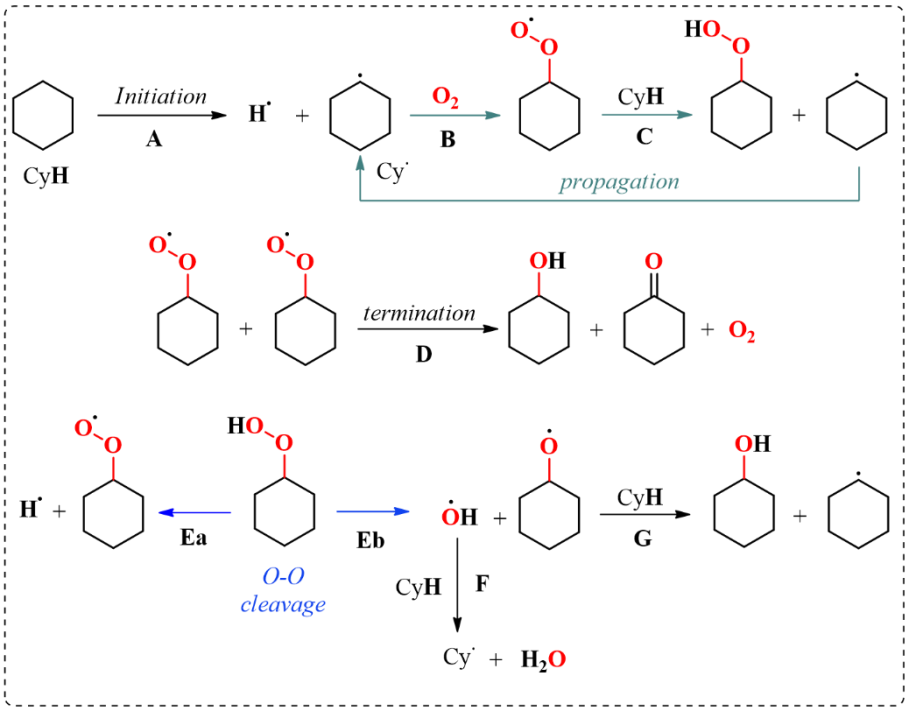

Scheme 3. Road map of the elementary reactions involved in the aerobic oxidation of cyclohexane.

EPR spin trapping for the CHHP decomposition by cobalt clusters 1-6

CHHP decomposition can be controlled by radical mechanism, therefore, the role of CHHP has been studied with the EPR spin-trapping method in order to correlate the catalytic activity of clusters **1-6** with the likely radical intermediates, as CHHP, involved in this reaction.[34,35] This is a well-stablished methodology, which relies on the trapping of short-lived radicals by a diamagnetic spin-trap molecule.[34] This reaction provides several stable spin adducts that can be detected by EPR spectroscopy.[36] In this sense, 5,5-dimethyl-1-pyrroline-*N*-oxide (DMPO) **7**, a well-known spin trap (Scheme 4), has been employed. The consequence of the reaction between DMPO and the intermediates involved in these reactions is the formation of several stable spin adducts such as **8**, **9** and **10**. In addition, these are persistent free radicals with a lifetime long enough to allow the identification by EPR spectroscopy.[37,38] The key to identify and quantify which species are formed in the reaction media is based on the different hyperfine couplings between the unpaired electron in the spin adduct and the H in the beta position of DMPO (through the a_N and a_H coupling constants).[34,39,40]

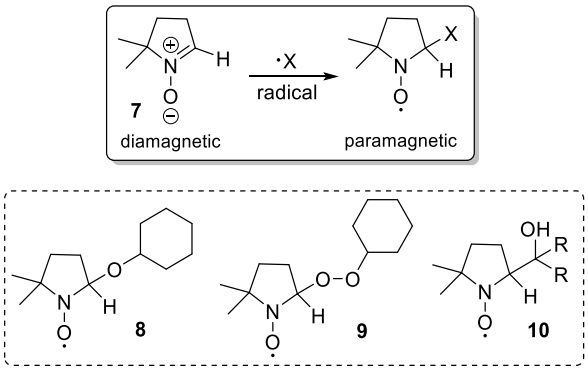

Scheme 4. Schematic illustration of the spin-trapping principle and structures of the spin adducts that can be detected in the reaction of DMPO and reaction intermediates.

The X-band CW EPR spectra obtained by using the spin-trap DMPO during the decomposition of CHHP with the several cobalt clusters **1**-**6** in cyclohexane are shown in Figures S22-S27. Two representatives EPR spin-adduct spectra, together with the combined simulation and deconvoluted single-spin-adduct species, are illustrated for clusters **2** and **5** in Figure 4.

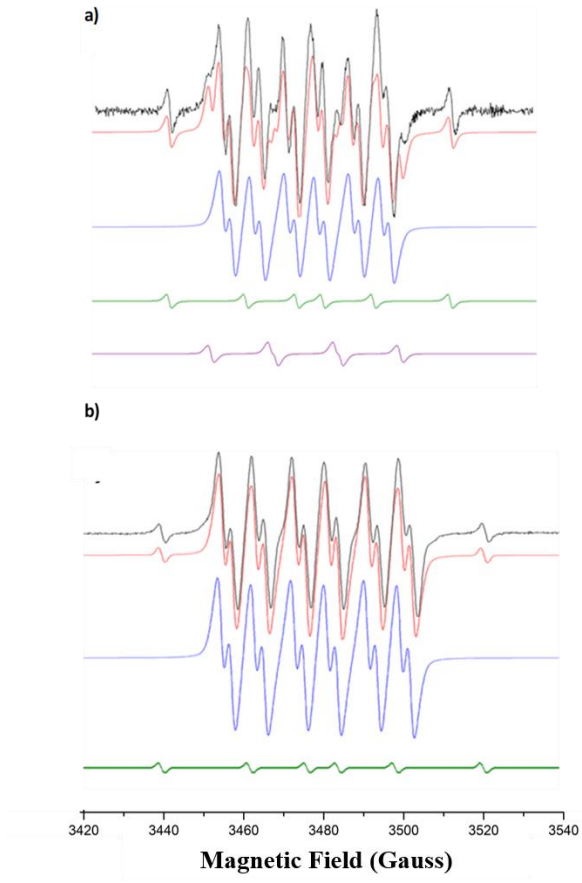

Figure 4. EPR spectrum and deconvoluted of DMPO spin adducts obtained during the decomposition of CHHP in cyclohexane in the presence of cobalt clusters **2** (a) or **5** (b). Experimental spectrum (black) and simulated spectrum (red), DMPO–O–C_6H_{11} spin adduct (blue), carbon-centered adduct (green), which is possibly a DMPO@C(OH)R_2 species, and DMPO–O-O–C_6H_{11} adduct (purple).

For cluster **2** (Figure 4a), the simulation of the spectrum and the comparison with literature values constitute the methodology employed to identify the following species: a DMPO–O–C_6H_{11} spin adduct, **8**, (a_N= 13.37, $a_{H(\beta)}$ = 5.95, $a_{H(\gamma)}$ = 1.91 G),[41] a DMPO-OO-C_6H_{11} adduct, **9**, (a_N= 14.46, a_H= 10.21 G)[42] and a carbon-centered adduct DMPO-C(OH)R_2, **10**, (a_N= 15.93, a_H= 21.31 G),[43] possibly originated from a ring-opening species, which could explain the formation of small amounts of adipic acid. The same strategy was employed for cluster **5** (Figure 4b). In this case it was possible to identify the following species: a DMPO–O–C_6H_{11} spin adduct, **8**, (a_N= 13.37, $a_{H(\beta)}$ = 5.95, $a_{H(\gamma)}$ = 1.91 G)[42] and a carbon-centered adduct DMPO-C(OH)R_2, **10**, (a_N= 15.93, a_H= 21.31 G).[43]

Furthermore, spin-trapping methodology is a semi-quantitative technique to determine the amount of spin adducts. The reason is that the absolute amount of adduct in solution is a result of several competing factors such as solvent, temperature, lifetime of the radical, and most important, the trapping reaction efficiency.[44] A semiquantitative analysis was carried out, with all the catalysts **1**-**6** tested under identical conditions; and consequently, any detected variations in the ratio among the studied radicals will be representative of different catalytic activities.[45]

Table 2 summarizes the relative abundances of spin adducts for CHHP decomposition by cobalt clusters **1**-**6**. An excess of DMPO-OR adducts has been detected compared with DMPO-OOR adducts, which is not be surprising, based on the fact that alkoxy radicals (RO$^{\bullet}$) are intrinsically more reactive than peroxy radicals (ROO$^{\bullet}$).[46] Hydrogen (H$^{\bullet}$) and hydroxy (HO$^{\bullet}$) radicals are supposed to be adsorbed in the cobalt oxo clusters, since these species were detected and isolated for cobalt cluster **1**.[25] On the one hand, the primary adduct DMPO–O–C_6H_{11}, **8**, is in a range from 74 to 98%. Therefore, there are significant variations in the relative amount of this species formed by using different cobalt clusters **1**-**6**. In addition, the large amount of alkoxy radicals explains the formation of an alcohol excess with respect to the ketone. On the other hand, DMPO–OO–C_6H_{11}, **9**, is not detected with cobalt cluster **5** while with the other catalysts it is in a range from 6 to 20 %. Cobalt clusters **1**-**3** (with acetate group) promote a higher ratio of these species with respect to cobalt clusters **4**-**6** (with benzoate group). In addition, catalysts with EWGs in the pyridine ring, with higher oxidation potentials, also promote a lower ratio of DMPO–OO–C_6H_{11}, **9**, in comparison with the ones that have an EDG in the pyridine ring. All cobalt clusters **1**-**6** promote small amounts of carbon centered adduct, **10**, from 2 to 7%. Finally, the three primary adducts detected, C_6H_{11}-O$^{\bullet}$, C_6H_{11}-OO$^{\bullet}$ and $C_6H_{11}^{\bullet}$ radicals, suggest that under the current catalytic conditions, it is likely that a general radical-based transformation is also occurring, as the one presented in Scheme 3 and Equations 1-8 in the Supporting Information.

Table 2. Relative abundances [%] of DMPO spin adducts obtained following CHHP decomposition in cyclohexane by cobalt clusters.

Entry	Catalyst	Nitroxide	$RO^{\cdot}$	$ROO^{\cdot}$	$C^{\cdot}$
1	Blank	--			
2	**1**	--	74	20	6
3	**2**	--	85	10	5
4	**3**	--	83	17	3
5	**4**	--	85	8	7
6	**5**	--	98	--	2
7	**6**	--	92	6	2

Oxygen transfer from CHHP to cyclohexane by cobalt clusters

Cyclohexane oxidation via oxygen transfer is a well-known reaction that can occur as a free-radical process over cobalt systems. CHHP is believed to be a key intermediate, which plays a main role in the formation of cyclohexanone or cyclohexanol (Scheme 3).[34,47,48] In fact, product distribution, related to A/K ratio, provides information of the process since in a free-radical process the A/K ratio is higher than 1 and in a radical process this ratio is lower than 1. Therefore, the autoxidation process by decomposition of CHHP to promote cyclohexanol and cyclohexanone is an accepted model, so it is considered in our study (see equations 1-8 in the SI). In this sense, a study to explore the mechanistic insight underlying the observed behavior for our cubane catalysts was carried out. Then, cobalt clusters **1**-**6** have been catalytically tested in the oxidation of cyclohexane with cyclohexyl hydroperoxide as a primary oxidant (Table 3). This study is the starting point in the reasoning of the observed selectivity when cobalt clusters **1**-**6** are employed as catalysts in the aerobic cyclohexane oxidation (Figure 2, Table S3).

The results summarized in Table 3 indicate that the CHHP decomposition with alcohol formation during the aerobic oxidation, is higher than 50% with all the catalysts used. However, there are two main differences among them. One is related to the A/K ratio, which is always higher for clusters **2** and **5** that contain an EWG in the pyridine ring. The other, and more important, is that EWGs promote higher oxygen transfer and lower oxidative dehydrogenation during the CHHP decomposition than EDG (see right column in Table 3). Finally, all these data support that cluster **5** is the most active and selective catalyst of this series not only for the direct oxidation but also for oxygen transfer from CHHP to cyclohexane.

Table 3. Summary of the catalytic activity (conversion and product distribution) of cobalt catalysts for cyclohexane oxidation employing CHHP as primary oxidant. Reaction conditions: 2.874 g cyclohexane (34.17 mmol) and 0.126 mg CHHP (1.08 mmol); 6 ppm Co (cobalt clusters **1**-**6)**; Tª 130 ºC; reaction time 1 hour; 6 bar (N_2).

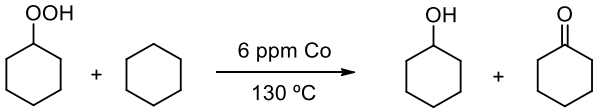

Entry	Catalyst	Conversion (%)	Selectivity (%)			Efficiency[d]
			A[a]	K[b]	Total[c]	
1	Blank	1	32	68	100	1.05
2	**1**	51	67	33	100	1.63
3	**2**	54	72	28	100	1.78
4	**3**	50	68	32	100	1.40
5	**4**	54	69	31	100	1.68
6	**5**	55	79	21	100	1.85
7	**6**	54	69	31	100	1.52

[a] A = alcohol, cyclohexanol; [b] K = ketone, cyclohexanone; [c] Total observed selectivity; [d] Products obtained from oxygen transfer and CHHP decomposition. In this sense, a value of 1 implies only CHHP decomposition while a value higher than 1 implies that the catalyst is able to decompose CHHP and oxidize cyclohexane at the same time (see Scheme S1).

In-situ Raman Spectroscopy employing molecular oxygen

In-situ Raman spectroscopy was used to elucidate the nature of the oxygen species formed on the cobalt clusters following a protocol previously introduced by Corma's group.[49] When oxygen was introduced in the Raman cell containing a sample of cobalt cluster pretreated with Ar, new Raman bands were observed. Indeed, the shift of the Raman bands depends on the nature of the cobalt cluster, which could be clearly correlated with oxidation potential of each one. In fact, the clusters with oxidation potentials lower than 0.74 V (**1**, **3** and **6**) promote oxygen species Co-O, based on the bands that appear in the range of 684 to 472 cm^{-1} as can be seen in Figure 5 (see Figures S28, S30 and S32, respectively for complete spectra),[50] which implies O-O bond cleavage.

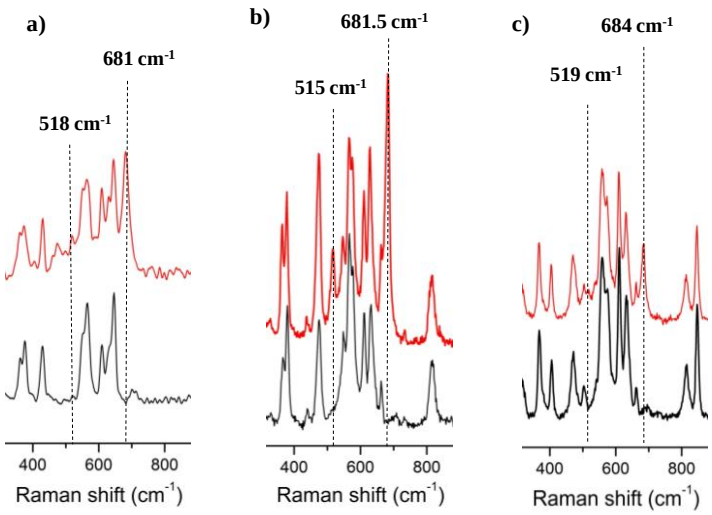

Figure 5. Raman spectra of complexes **1** (a), **3** (b) and **6** (c) between 850 and 350 cm^{-1} in Ar (black) and passing an O_2 flow (red).

On the other hand, clusters with oxidation potentials higher than 0.78 V (**2**, **4** and **5**) promote oxygen species Co-O-O, based on the bands that appear in the range of 1600 to 858 cm^{-1}, which means that O-O bond is not cleaved (Figure 6). Moreover, the oxygen species formed with clusters (**2**, **4** and **5**) are not identical. In this sense, clusters **2** and **4**, show Raman bands at 1261 and 1285 cm^{-1}, respectively, which are shown in Figure 6 (see Figures S29 and S31, respectively, for complete spectra). These bands are assigned to $O_2^{\delta-}$ ($0 < \delta < 1$) adspecies.[50–52]

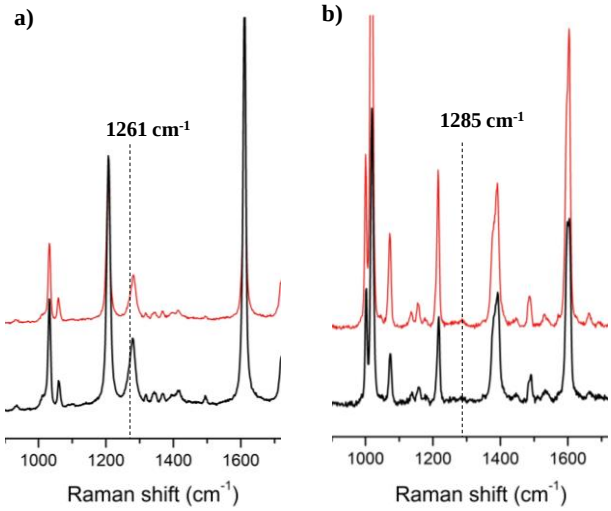

Figure 6. Raman spectra of complexes **2** (a) and **4** (b) between 1700 and 900 cm^{-1} in Ar (black) and passing an O_2 flow (red).

Finally, cluster **5,** with the highest oxidation potential associated (0.956 V) presents a totally different behavior. In this case absorption of molecular oxygen is observed (1600 cm^{-1}),[50] bands at 1159, 1138 and 1107 cm^{-1} are assigned to η^1 superoxide species (Figure 7)[50,53,54] and the band at 858 cm^{-1} is assigned to nonplanar bridging peroxide species (Figure 7).[43–47]

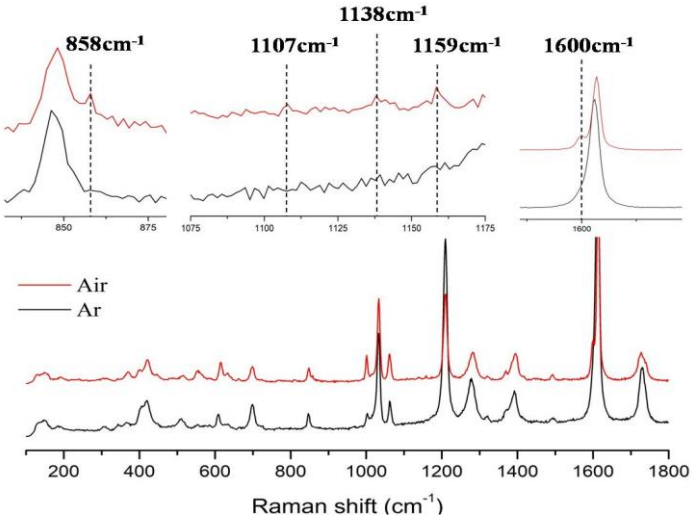

Figure 7. Raman spectra of complex **5** in Ar (black) and passing an O_2 flow (red).

From these results, it can be concluded that catalysts with higher oxidation potential promote more selective species than the ones with lower oxidation potential. As a final result from these data, it can be highlighted that the activation of oxygen bonds to provide peroxide and superoxide species is the best way to oxidize inactivated CH bonds in alkanes.

Influence of the Cobalt Cluster Nature in the whole Mechanism

Scheme 3 illustrates the well-established mechanism of the cyclohexane oxidation. Based on previous results obtained by experimental data and *in situ* studies, a mechanism combining aerobic oxidation with oxygen transfer for cobalt clusters **1-6** (Scheme 5) has been proposed. This Scheme combines the elementary reactions illustrated in Scheme 3 with the identified intermediates over cobalt clusters, in order to correlate the role of each cobalt core and its electronic properties with the reaction pathway. Considering the observed species, it can be appreciated that catalysts are involved in two different parts of the process: in molecular oxygen activation and in CHHP activation. Thus, both are clearly related to the O-O bond interaction of each mentioned molecule with the cobalt clusters.

Related to O_2 activation, the main role of the developed clusters is in the initiation step. However, according to the species detected by *in situ* Raman spectroscopy, these catalysts can be clearly classified in two groups: one with O-O bond cleavage activation (including clusters **1**, **3** and **6**) and the other, where the O-O bond is not cleaved (including clusters **2**, **4** and **5**). This fact indicates that clusters **1**, **3** and **6** follow reactions **Aa** and **B**, and finally propagation **D** (left way Scheme 5). While clusters **2**, **4** and **5** are involved in the reactions **Ab** and **C**, and finally also propagation **D** (right way Scheme 5).

The behavior of these six cobalt clusters for CHHP decomposition is quite similar, mainly observing alkoxy radical as major specie by EPR experiments. Thus, reactions **Ea** and **Eb** (Scheme 5) are followed by all the catalysts except for cluster **5**, which promotes exclusively alkoxy radicals, and therefore, follows **Eb**. In addition, these cobalt clusters can adsorb the hydroxy radical blocking its high reactivity, which could damage selectivity, as it was observed during OER process.[25] Finally, the study of oxygen transfer reactions (oxidation of CyH with CHHP to generate A/K) supports that clusters **2** and **5** have a major contribution in the propagation reaction, while clusters **3** and **6** play a minor role in this process. Therefore, the influence of these clusters in the oxygen transfer reaction during cyclohexane oxidation is also correlated with its electron density.

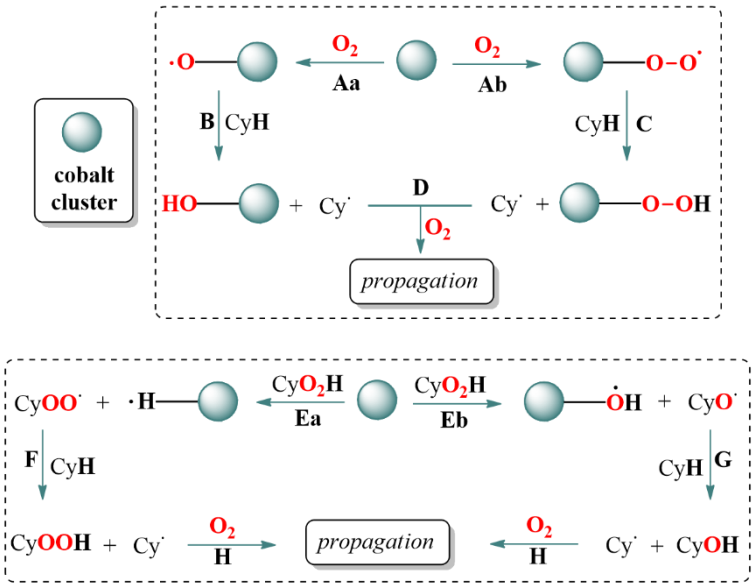

Scheme 5. Proposed mechanism for cyclohexane oxidation employing cobalt cluster catalysts. O_2 activation (up) and CHHP decomposition (down).

3. Conclusions

A family of cobalt clusters, where the electronic properties of the $[Co_4O_4]$ core can be modulated with the organic ligands, has been reported. In addition, a new straightforward synthetic strategy based on the pK_b of different carboxylate ligands has also been described. These cobalt clusters have shown high activity and selectivity as catalysts in cyclohexane oxidation in neat conditions with N_2 enriched air (with only 5% of O_2) as primary oxidant. For this reaction, the electronic properties of the catalysts can be correlated with the catalytic activity. In addition, these catalysts also promote oxygen transfer from CHHP to cyclohexane during the aerobic oxidation. For these reactions, a mechanistic insight has been achieved by using spin trapping experiments and experimental reactions. On one hand, spin trapping experiments suggest that a radical contribution takes place, where the most active and selective catalyst promotes almost exclusively alkoxy

radical species by reaction with hydroperoxide. On the other hand, experimental reactions with CHHP and cyclohexane in the presence of cobalt clusters suggest that CHHP decomposition to oxidize cyclohexane is mainly controlled by a non-radical process. In this sense, electronic density of these catalysts has a clear influence on the product distribution, which is correlated with the ratio of radical/non-radical contribution of the process. Finally, in-situ Raman spectroscopy was also employed to characterize the oxygen intermediate species formed on the cobalt clusters during the oxidation reaction. In fact, the promoted species in each case are related to the oxidation potential of the cobalt clusters.

To sum up, in this work we have carried out the synthesis of six cobalt clusters highly active and selective for cyclohexane oxidation reaction under neat conditions using enriched air as oxidant. In addition, the mechanistic study illustrates a global mechanism and highlights the contribution of the developed clusters in each single step of the whole process. Finally, the contribution of these cobalt clusters in each single reaction step is clearly correlated with their electron density.

Experimental Section

Experimental procedures employed during this study, Crystallographic parameters, Cyclic voltammograms, Raman spectra, kinetic and mechanistic studies are described in the Supporting Information.

Conflicts of interest

The authors declare no competing financial interest.

Acknowledgements

Authors thank Prof. A. Corma for his support and discussion on this work. S.G.T. thanks to MINECO for a FPU Ph.D. contract FPU16/02117. P.O-B. thanks the financial support by the Spanish Government (RTI2018-096399-A-I00). Authors would like to thank Ms. Carmen Clemente and Ms. Adelina Muñoz for the ESI-MS and Raman measurements, respectively. Authors would also like to thank the use of analytical facilities at the X-Ray Unit of RIAIDT (Universidad de Santiago de Compostela).

Notes and references

1 M. Eichelbaum, R. Glaum, M. Hävecker, K. Wittich, C. Heine, H. Schwarz, C. K. Dobner, C. Welker-Nieuwoudt, A. Trunschke and R. Schlögl, *ChemCatChem*, 2013, **5**, 2318–2329.

2 U. Schuchardt, D. Cardoso, R. Sercheli, R. Pereira, S. Rosenira, M. C. Guerreiro, D. Mandelli, E. V Spinacé and E. L. Pires, *Appl. Catal. A Gen.*, 2001, **211**, 1–17.

3 C. Hess, M. H. Looi, S. B. A. Hamid and R. Schlögl, *Chem. Commun.*, 2006, 451–453.

4 R. Y. Saleh, I. E. Wachs, S. S. Chan and C. C. Chersich, *J. Catal.*, 1986, **98**, 102–114.

5 P. Du, J. A. Moulijn and G. Mul, *J. Catal.*, 2006, **238**, 342–352.

6 Z. Tian, A. Fattahi, L. Lis and S. R. Kass, *J. Am. Chem. Soc.*, 2006, **128**, 17087–17092.

7 R. H. Crabtree, *Chem. Rev.*, 1995, **95**, 987–1007.

8 Y. Ishii, S. Sakaguchi and T. Iwahama, *Adv. Synth. Catal.*, 2001, **343**, 393–427.

9 J. M. Brégeault, *Dalt. Trans.*, 2003, **3**, 3289–3302.

10 U. Schuchardt, W. A. Carvalho and E. V. Spinach, *Synlett*, 1993, 713–718.

11 B. Retcher, J. S. Costa, J. Tang, R. Hage, P. Gamez and J. Reedijk, *J. Mol. Catal. A Chem.*, 2008, **286**, 1–5.

12 X. H. Lu, H. X. Yuan, J. Lei, J. L. Zhang, A. A. Yu, D. Zhou and Q. H. Xia, *Indian J. Chem. - Sect. A*, 2012, **51A**, 420–427.

13 T. F. S. Silva, T. C. O. M. Leod, L. M. D. R. S. Martins, M. F. C. Guedes Da Silva, M. A. Schiavon and A. J. L. Pombeiro, *J. Mol. Catal. A Chem.*, 2013, **367**, 52–60.

14 N. V. Maksimchuk, K. A. Kovalenko, V. P. Fedin and O. A. Kholdeeva, *Chem. Commun.*, 2012, **48**, 6812–6814.

15 A. R. Kim, S. Ahn, T. U. Yoon, J. M. Notestein, O. K. Farha and Y. S. Bae, *ChemCatChem*, 2019, **11**, 5650–5656.

16 M. P. De Almeida, L. M. D. R. S. Martins, S. A. C. Carabineiro, T. Lauterbach, F. Rominger, A. S. K. Hashmi, A. J. L. Pombeiro and J. L. Figueiredo, *Catal. Sci. Technol.*, 2013, **3**, 3056–3069.

17 Y. Xiao, J. Liu, K. Xie, W. Wang and Y. Fang, *Mol. Catal.*, 2017, **431**, 1–8.

18 L. Chen, Y. Zhou, Z. Gui, H. Cheng and Z. Qi, *J. Mater. Sci.*, 2017, **52**, 7186–7198.

19 P. Wu, Y. Cao, Y. Wang, W. Xing, Z. Zhong, P. Bai and Z. Yan, *Appl. Surf. Sci.*, 2018, **457**, 580–590.

20 L. M. D. R. S. Martins, A. Martins, E. C. B. A. Alegria, A. P. Carvalho and A. J. L. Pombeiro, *Appl. Catal. A Gen.*, 2013, **464**–**465**, 43–50.

21 J. K. Beattie, T. W. Hambley, J. A. Klepetko, A. F. Masters and P. Turner, *Polyhedron*, 1998, **17**, 1343–1354.

22 S. Gutiérrez-Tarriño, J. L. Olloqui-Sariego, J. J. Calvente, G. M. Espallargas, F. Rey, A. Corma and P. Oña-Burgos, *J. Am. Chem. Soc.*, 2020, **142**, 19198–19208.

23 S. Gutiérrez Tarriño, J. L. Olloqui-Sariego, J. J. Calvente, M. Palomino, G. Minguez Espallargas, J. L. Jorda, F. Rey and P. Oña-Burgos, *ACS Appl. Mater. Interfaces*, 2019, **11**, 46658.

24 N. S. McCool, D. M. Robinson, J. E. Sheats and G. C. Dismukes, *J. Am. Chem. Soc.*, 2011, **133**, 11446–11449.

25 A. I. Nguyen, M. S. Ziegler, P. Oña-Burgos, M. Sturzbecher-Hohne, W. Kim, D. E. Bellone and T. D. Tilley, *J. Am. Chem. Soc.*, 2015, **137**, 12865–12872.

26 I. G. Denisov, T. M. Makris, S. G. Sligar and I. Schlichting, *Chem. Rev.*, 2005, **105**, 2253–2277.

27 R. Chakrabarty, S. J. Bora and B. K. Das, *Inorg. Chem.*, 2007, **46**, 9450–9462.

28 S. Berardi, G. La Ganga, M. Natali, I. Bazzan, F. Puntoriero, A. Sartorel, F. Scandola, S. Campagna and M. Bonchio, *J. Am. Chem. Soc.*, 2012, **134**, 11104–11107.

29 A. Karmakar, R. J. Sarma and J. B. Baruah, *Polyhedron*, 2007, **26**, 1347–1355.

30 R. Chakrabarty, P. Sarmah, B. Saha, S. Chakravorty and B. K. Das, *Inorg. Chem.*, 2009, **48**, 6371–6379.

31 R. Chakrabarty, P. Sarmah, B. Saha, S. Chakravorty and B. K. Das, *Inorg. Chem.*, 2009, **48**, 6371–6379.

32 R. Chakrabarty, S. J. Bora and B. K. Das, *Inorg. Chem.*, 2007, **46**, 9450–9462.

33 A. I. Nguyen, J. Wang, D. S. Levine, M. S. Ziegler and T. D. Tilley, *Chem. Sci.*, 2017, **8**, 4274–4284.

34 X. Liu, M. Conte, Q. He, D. W. Knight, D. M. Murphy, S. H. Taylor, K. Whiston, C. J. Kiely and G. J. Hutchings, *Chem. - A Eur. J.*, 2017, **23**, 11834–11842.

35 C. M. Jones and M. J. Burkitt, *J. Am. Chem. Soc.*, 2003, **125**, 6946–6954.

36 M. Conte, K. Wilson and V. Chechik, *Org. Biomol. Chem.*, 2009, **7**, 1361–1367.

37 M. Conte, K. Wilson and V. Chechik, *Rev. Sci. Instrum.*, , DOI:10.1063/1.3492247.

38 M. Conte, X. Liu, D. M. Murphy, S. H. Taylor, K. Whiston and G. J. Hutchings, *Catal. Letters*, 2016, **146**, 126–135.

39 E. Finkelstein, G. M. Rosen and E. J. Rauckman, *J. Am. Chem. Soc.*, 1980, **102**, 4994–4999.

40 D. R. Duling, *J. Magn. Reson. Ser. B*, 1994, 104, 105–110.

41 S. L. Baum, I. G. M. Anderson, R. R. Baker, D. M. Murphy and C. C. Rowlands, *Anal. Chim. Acta*, 2003, **481**, 1–13.

42 M. J. Davies and T. F. Slater, *Biochem. J.*, 1986, **240**, 789–795.

43 E. G. Janzen, C. A. Evans and J. I. P. Liu, *J. Magn. Reson.*, 1973, **9**, 513–516.

44 P. Ionita, M. Conte, B. C. Gilbert and V. Chechik, *Org. Biomol. Chem.*, 2007, **5**, 3504–3509.

45 M. Conte, H. Miyamura, S. Kobayashi and V. Chechik, *J. Am. Chem. Soc.*, 2009, **131**, 7189–7196.

46 B. W. Griffin, *Can. J. Chem.*, 1982, **60**, 1463–1473.

47 I. Hermans, P. Jacobs and J. Peeters, *Chem. - A Eur. J.*, 2007, **13**, 754–761.

48 B. P. C. Hereijgers and B. M. Weckhuysen, *J. Catal.*, 2010, **270**, 16–25.

49 J. Guzman, S. Carrettin and A. Corma, *J. Am. Chem. Soc.*, 2005, **127**, 3286–3287.

50 D. Nguyen, G. Kang, N. Chiang, X. Chen, T. Seideman, M. C. Hersam, G. C. Schatz and R. P. Van Duyne, *J. Am. Chem. Soc.*, 2018, **140**, 5948–5954.

51 E. A. Pozzi, M. D. Sonntag, N. Jiang, N. Chiang, T. Seideman, M. C. Hersam and R. P. Van Duyne, *J. Phys. Chem. Lett.*, 2014, **5**, 2657–2661.

52 N. Jiang, E. T. Foley, J. M. Klingsporn, M. D. Sonntag, N. A. Valley, J. A. Dieringer, T. Seideman, G. C. Schatz, M. C. Hersam and R. P. Van Duyne, *Nano Lett.*, 2012, **12**, 5061–5067.

53 R. Zhang, Y. Zhang, Z. C. Dong, S. Jiang, C. Zhang, L. G. Chen, L. Zhang, Y. Liao, J. Aizpurua, Y. Luo, J. L. Yang and J. G. Hou, *Nature*, 2013, **498**, 82–86.

54 J. Steidtner and B. Pettinger, *Phys. Rev. Lett.*, 2008, **100**, 1–4.

Table of Contents

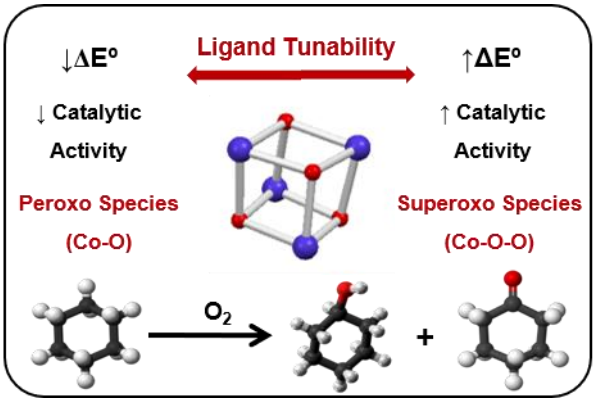

Well-defined tetranuclear cobalt coordination compounds with modulable electron density as active and selective catalysts for aerobic cyclohexane oxidation.